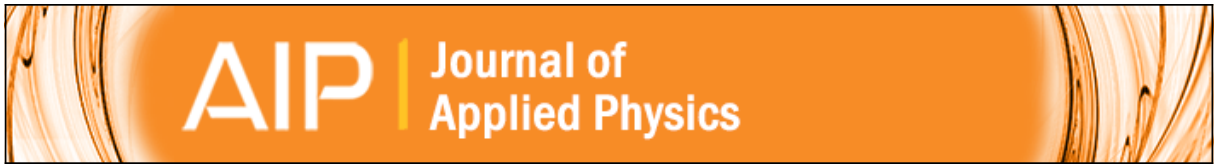

Enhancement in electron field emission in ultrananocrystalline and microcrystalline diamond films upon 100 MeV silver ion irradiation

Huang-Chin Chen, Umesh Palnitkar, Way-Faung Pong, I-Nan Lin, Abhinav Pratap Singh, and Ravi Kumar

Citation: Journal of Applied Physics **105**, 083707 (2009); doi: 10.1063/1.3106638

View online: http://dx.doi.org/10.1063/1.3106638

View Table of Contents: http://scitation.aip.org/content/aip/journal/jap/105/8?ver=pdfcov

Published by the AIP Publishing

Enhancement in electron field emission in ultrananocrystalline and microcrystalline diamond films upon 100 MeV silver ion irradiation

Huang-Chin Chen,[1] Umesh Palnitkar,[1] Way-Faung Pong,[1] I-Nan Lin,[1,a)] Abhinav Pratap Singh,[2] and Ravi Kumar[2]
[1]*Department of Physics, Tamkang University, Tamsui, Taiwan 251, Republic of China*
[2]*Inter-University Accelerator Center, Aruna Asaf Ali Marg, New Delhi 110007, India*

(Received 30 December 2008; accepted 21 February 2009; published online 21 April 2009)

Enhanced electron field emission (EFE) behavior was observed in ultrananocrystalline diamond (UNCD) and microcrystalline diamond (MCD) films upon irradiation with 100 MeV Ag^{9+}-ions in a fluence of 5×10^{11} ions/cm^2. Transmission electron microscopy indicated that while the overall crystallinity of these films remained essentially unaffected, the local microstructure of the materials was tremendously altered due to heavy ion irradiation, which implied that the melting and recrystallization process have occurred along the trajectory of the heavy ions. Such a process induced the formation of interconnected nanocluster networks, facilitating the electron conduction and enhancing the EFE properties for the materials. The enhancement in the EFE is more prominent for MCD films than that for UNCD films, reaching a low turn-on field of $E_0=3.2$ V/μm and large EFE current density of $J_e=3.04$ mA/cm^2 for 5×10^{11} ions/cm^2 heavy ion irradiated samples.
 [DOI: 10.1063/1.3106638]

I. INTRODUCTION

Diamond films have been extensively investigated for their application as electron field emitters, owing to their negative electron affinity and low effective work function.[1,2] While the physical properties are found to depend on the crystallinity of the materials, the electrical and optical characteristics of the films are more closely related to the microstructure of the samples.[3] When moving from microcrystalline diamond (MCD) toward nanocrystalline diamond (NCD), the grain size decreases such that the H content and the amount of the graphitic inclusions in the grain boundaries increase.[3–5] The hydrogens are presumed to reside at the grain boundaries, saturating the dangling bonds.[6] There are studies on the correlation of hydrogen retention with the bonding,[5–7] conductivity,[8] and field emission[9,10] of diamond films as a function of grain size. However the reports on whether the hydrogen incorporation within the structure of diamond will increase or decrease the conductivity of the materials are controversial. On the other hand, the sp^2-bonded carbons within the chemical vapor deposition (CVD) diamond films can be thought of as a conduction promoter, particularly if the sp^2-bonds form interconnected networks along which electrons are free to move.[6]

While the hydrogen content in the diamond films can be controlled by postannealing process, the control on the proportion of sp^2-bonds is not as reliable. Irradiation by energetic heavy ions into the diamond films can break the C–C bonds under controlled manner and, therefore, become an efficient and reliable way for controlling the proportion of sp^2-bonds in the materials. There are many reports that discuss the effects of ion beam irradiation on the characteristics of type IIa diamond,[11] diamondlike carbon film,[12] tetrahedral amorphous C,[13] graphite,[14] polycrystalline CVD diamond,[15–17] etc. Furthermore, Pandey *et al.*[18] and Koinkar *et al.*[19] studied the field emission enhancement by swift heavy ions irradiation in CVD diamonds, but the mechanism is still not clear.

Here we report the effect of heavy ion (100 MeV Ag^{9+}) irradiation on changing the morphology and improving the electron field emission (EFE) properties of the diamond films. The modification of the microstructure of these films due to heavy ion irradiation was investigated in detail using transmission electron microscopy (TEM), and the correlation of these characteristics with the resulted EFE characteristics was discussed.

II. EXPERIMENTALS

The ultra-NCD (UNCD) films were grown on silicon substrates by Ar-plasma based microwave plasma enhanced chemical vapor deposition (MPECVD) process using IPLAS-Cyrannus reactor.[20] They were grown in (1% CH_4)/Ar plasma (100 SCCM) (SCCM denotes standard cubic centimeter at STP) at 1200 W and 120 torr for 3 h to reach a thickness of about 300 nm. The substrate temperature was estimated to be around 400 °C during the growth of UNCD films. In contrast, MCD films of ~1 μm thickness were deposited on silicon substrates by the H_2-plasma based MPECVD process, using an ASTex 5400 reactor. The (5.0%)CH_4/H_2 gas mixture with flow rates of 5/95 SCCM (Ref. 21) was excited by 1500 W microwaves (2.45 GHz), while the total pressure in the chamber was maintained at 55 torr (growth time of 90 min). The substrate temperature was estimated to be around 900 °C during the growth of MCD films.

The diamond films were subjected to heavy ion irradiation using 100 MeV Ag^{9+}-ions from 15 MV Pelletron accelerator at Inter-University Accelerator Centre, New Delhi,

a)Author to whom correspondence should be addressed. Electronic mail: inanlin@mail.tku.edu.tw.

India.[17–19] The current was ~1 pnA, which is equivalent to 6.2×10^9 ions/s. The samples were mounted inside the scattering chamber, which was evacuated to base pressure of 1×10^{-6} torr. The samples were irradiated with fluences of 5×10^{10} or 5×10^{11} ions/cm^2. The 100 MeV silver ions have a projected range of 7.68 μm and longitudinal straggling of 230.3 nm as simulated with SRIM-2008.[22] Therefore, the Ag^{9+}-ions will pass through the diamond films and get buried deep into the substrate for all the samples. The sole effect of heavy ion irradiation is to induce the atomic defects for the UNCD and MCD films, and there is no Ag^{9+}-ions doping effect on the films. The ions have an electronic energy loss of 2.194×10^4 eV/nm and nuclear energy loss of 93.18 eV/nm, indicating that the ions will lose energy mostly by electronic excitations in diamond. The lattice damage effects of nuclear energy loss will be minimal.

The films were characterized using scanning electron microscopy (SEM: JEOL JSM-6500F), TEM (JOEL, 2100), Raman spectroscopy (Renishaw, 514.5 nm), x-ray photoelectron spectroscopy (XPS, PHI, 1600), and near edge x-ray absorption fine structure spectroscopy (NEXAFS). EFE properties of the diamond films were measured with a tunable parallel plate setup in which the sample-to-anode distance was varied using a micrometer. The current-voltage (*I-V*) characteristics were measured using an electrometer (Keithley 237) under pressures below 10^{-6} torr, where the maximum available voltage of the setup was 1100 V and the current was restricted to 10 mA. The EFE parameters were extracted from the obtained *I-V* curves by using the Fowler–Nordheim (FN) model,[23] where the turn-on field was designated as the intersection of the lines extrapolated from the low field and high field segments of the FN plot.

III. RESULTS AND DISCUSSION

Figures 1(a) and 1(b) show, respectively, the SEM micrographs for UNCD and MCD samples. The UNCD samples contain grains of the sizes less than 10 nm and roundish in morphology, whereas the MCD samples consist of grains about 300–500 nm in size and faceted in geometry. Figure 2, the typical TEM micrographs of UNCD films, and the inset of Fig. 2, the enlarged micrograph of designated region [inset (a), Fig. 2], reveal that the UNCD grains (~5–10 nm) are very uniform in size. The selected area diffraction (SAD) patterns [inset (b) of Fig. 2] indicate that these films are diamonds. The SAD almost forms a continuous ring, the characteristic of ultrasmall and randomly oriented grains. In contrast, TEM micrographs in Fig. 3 and low magnification micrographs [inset (a), Fig. 3] indicate that the MCD diamond grains are essentially featureless. The SAD [inset (b), Fig. 3] shows spotty rings, a characteristic of large grain materials.

Figures 4(a) and 4(b) show Raman spectra for UNCD and MCD films, respectively. For as-deposited UNCD films, the Raman peaks are very diffuse, and no sharp *D*-band (at 1333 cm^{-1}) is observable [solid line, Fig. 4(a)], which is presumably due to the smallness of the grain size. The 1144 cm^{-1} (υ_1-band) and 1480 cm^{-1} (υ_2-band) Raman peaks are assigned as vibrations from transpolyacetylene

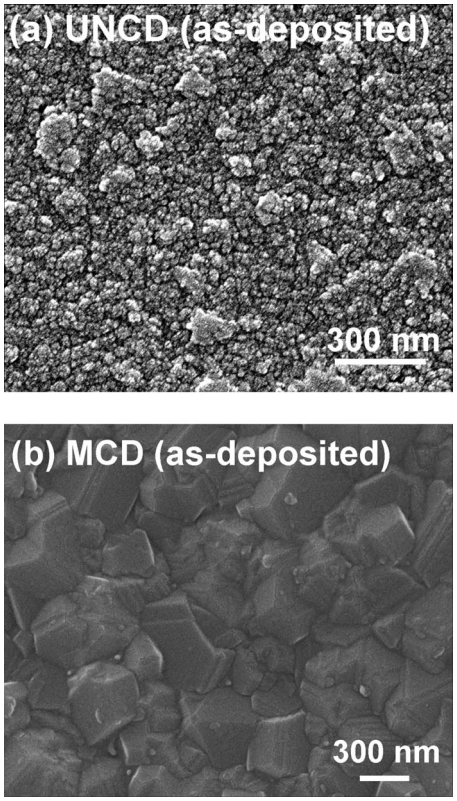

FIG. 1. SEM micrographs of as-deposited (a) UNCD films, which were grown under 99% Ar (1% CH_4) plasma, and (b) MCD films, which were grown under 95% H_2 (5% CH_4) plasma.

groups presenting at the grain boundaries.[24] The 1343 cm^{-1} (D^*-band) Raman peak is assigned as disordered sp^3 bonds and the 1580 cm^{-1} (*G*-band) corresponds to graphite peak.[25] In contrast, solid line in Fig. 4(b) shows that the MCD films are predominated with a sharp 1333 cm^{-1} Raman peak (*D*-band) corresponding to *F*2*g* zone center optical phonon of diamond.

To more clearly examine the bonding nature of these films, NEXAFS were performed and the results are shown in Fig. 4(c), where the NEXAFS corresponding to single crystal diamond is included as standard to facilitate the comparison [curve I, Fig. 4(c)]. This figure reveals a sharp rising edge at

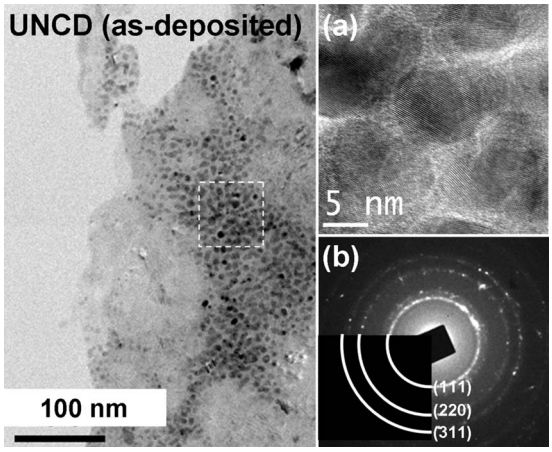

FIG. 2. TEM micrographs of as-deposited UNCD films, which were grown under 99% Ar (1% CH_4) plasma.

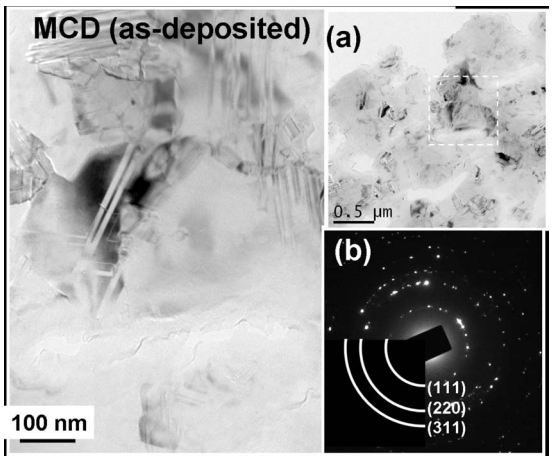

FIG. 3. TEM micrographs of as-deposited MCD films, which were grown under 95% H_2 (5% CH_4) plasma.

289.7 eV ($C1s$ σ^*-band), and a large deep at 302.5 eV is observed for both UNCD and MCD films, which are the signatures of the diamond materials.[26,27] These NEXAFS confirm, again, that both the UNCD and MCD films are diamonds, although, for UNCD films, the $C1s$ σ^*-edge is not as sharp and the 302.5 eV valley is not as deep as that for standard diamond. In addition, there appears a small peak at 285.5 eV corresponding to $C1s$ π^*-bond in the NEXAFS of UNCD films, implying that there contains small proportion of sp^2-bonded carbon materials in the films, which are presumed to reside in grain boundaries.[28] There is no π^*-bond observable for MCD films.

Figure 5 shows the modification in the EFE characteristics of the UNCD and MCD films due to Ag^{9+}-ion irradiation. The insets in these figures show the FN plots used for analyzing the EFE characteristics. The high field segment of the FN plot fits a straight line, indicating that the FN model can explain these EFE characteristics very well. The details of the field emission parameters, such as turn-on field (E_0) and EFE current density (J_e), are given in Table I. For the as-deposited UNCD films, the EFE process can be turned on at a field of $(E_0)_{UNCD}=13.51$ V/μm [curve I, Fig. 5(a)], which is smaller than that for as-deposited MCD samples [$(E_0)_{MCD}=28.0$ V/μm, curve I in Fig. 5(b)]. Probably, it is the smaller and defective grains contained in UNCD films that result in larger proportion of grain boundaries and more abundant intermediate energy levels, giving rise to better field emission behavior.[20] However, both of the as-deposited films possess very small EFE current density, viz., J_e is 2.34×10^{-4} mA/cm^2 for UNCD films and 1.96×10^{-6} mA/cm^2 for MCD films at the applied field of $E_a=20$ V/μm.

The 100 MeV Ag^{9+}-ion irradiation markedly improves the EFE characteristics of these samples. The turn-on field decreases with increasing ion irradiation fluence. The $(E_0)_{UNCD}$ decreases from 13.51 to 6.44 V/μm for UNCD films, and the $(E_0)_{MCD}$ decreases from 28.0 to 3.2 V/μm for MCD films due to 5×10^{11} Ag^{9+}-ion irradiation (Fig. 5 and Table I). The ultimate EFE current density achieved with the dosage of 5×10^{11} ion/cm^2 is $(J_e)_{UNCD}=0.351$ mA/cm^2 for UNCD films and $(J_e)_{MCD}=3.20$ mA/cm^2 for MCD films. It

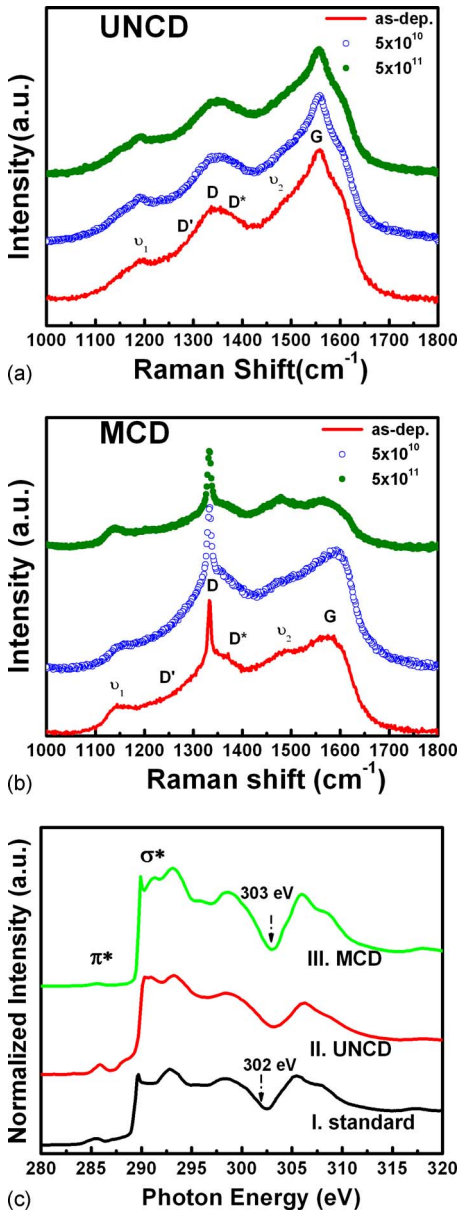

FIG. 4. (Color online) [(a) and (b)] Raman spectra for as-deposited and 100 MeV Ag^{9+}-ion irradiated (a) UNCD and (b) MCD samples. (c) The NEXAFS of as-deposited UNCD and MCD films along with the NEXAFS from single crystalline diamond films.

is interesting to observe that a smaller reduction in the turn-on field for emission is observed for UNCD films that had lower turn-on field before irradiation and a larger reduction in the turn-on field for emission is observed for MCD films that had higher turn-on field before irradiation.

To understand the factor resulting in pronounced improvement in the EFE properties for these films, the Ag^{9+}-ion irradiated films were examined using Raman and NEXAFS spectroscopies. Raman spectra shown in Figs. 4(a) and 4(b) reveal that the respective characteristics for UNCD and MCD samples are not markedly changed up to 5×10^{11} ions/cm^2 Ag^{9+}-ion irradiation. NEXAFS spectra shown in Figs. 6(a) and 6(b) for UNCD and MCD films, respectively, also indicate that the signature of diamonds, $C1s$ σ^*-bond at 289.7 eV and deep-valley at 302.5 eV, are not significantly altered due to 100 MeV Ag^{9+}-ion irradia-

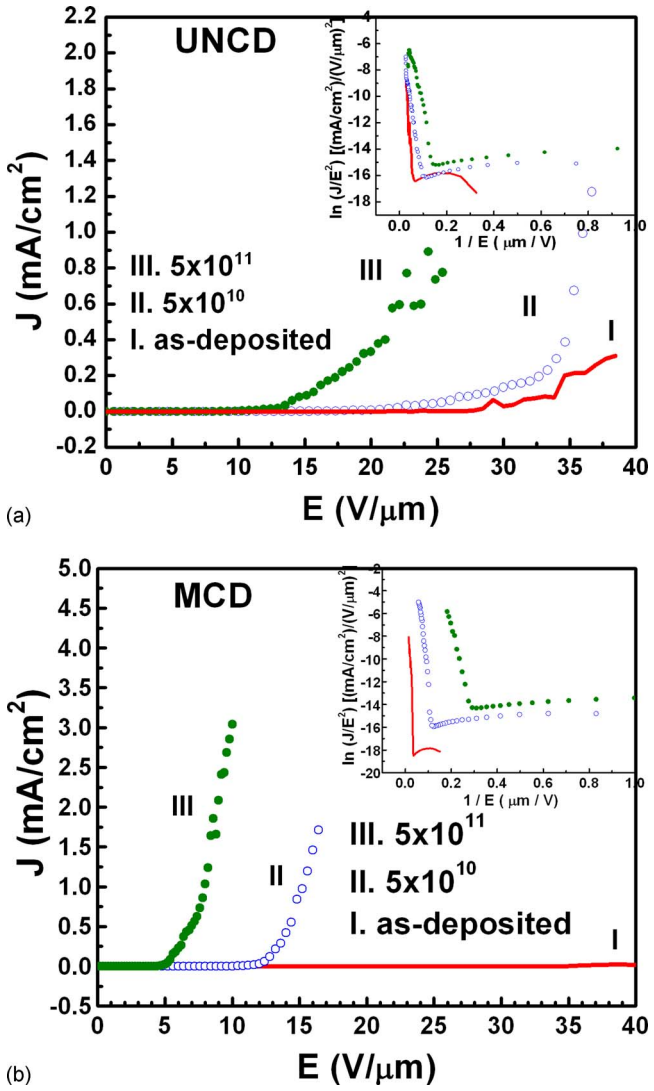

FIG. 5. (Color online) EFE property of (a) UNCD and (b) MCD samples before and after irradiation with 100 MeV Ag^{9+}-ions at various fluences. The insets show the FN plots.

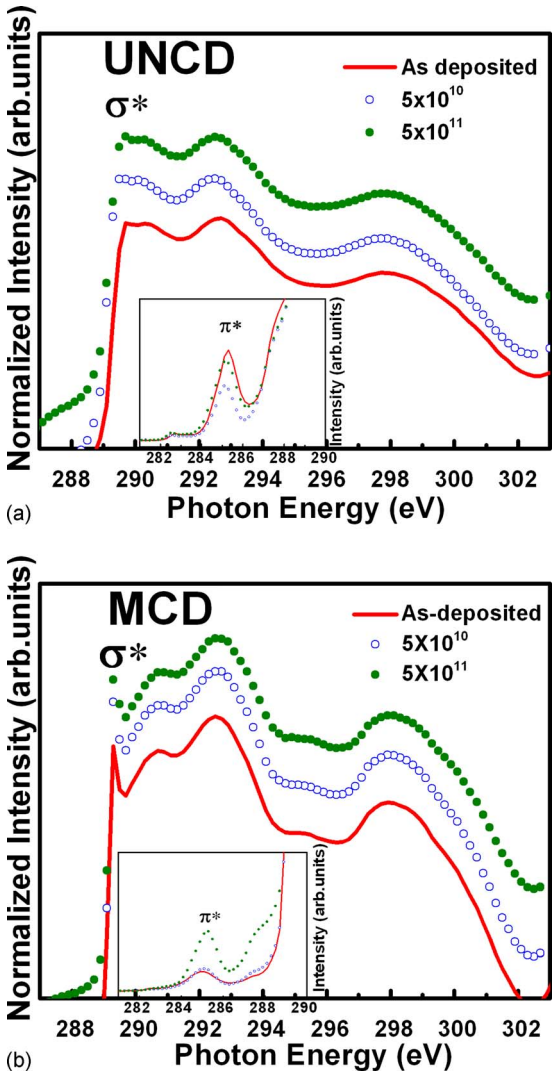

FIG. 6. (Color online) The NEXAFS for as-deposited and 100 MeV Ag^{9+}-ion irradiated (a) UNCD and (b) MCD films.

tion. These observations imply that the dosage of 5×10^{11} ions/cm^2 experienced by the films is still below the critical dosage required to induce marked modification on the crystallinity of the diamonds.[17–19]

TABLE I. EFE characteristics of UNCD and MCD materials irradiated with 100 MeV Ag^{9+} ions. The UNCD materials were grown in CH_4/Ar plasma, whereas the MCD materials were grown in CH_4/H_2 plasma.

Sample	Fluence (ions/cm^2)	Turn-on field[a] E_0 (V/μm)	EFE current density[b] J_e (mA/cm^2)
UNCD	As-dep.	13.51	2.3×10^{-4}
	5×10^{10}	9.78	0.97×10^{-3}
	5×10^{11}	6.44	0.351
MCD	As dep.	28.00	1.96×10^{-6}
	5×10^{10}	8.00	1.41×10^{-3}
	5×10^{11}	3.2	3.04

[a]E_0: turn-on field is designated as the intersection of the high-field and low-field segments in the FN plots.
[b]J_e: the field emission current density measured at 20 V/μm for UNCD and at 10 V/μm for MCD.

Furthermore, the Ag^{9+}-ion irradiation on the modification in the surface characteristics of the films is illustrated using XPS. Figure 7(a) shows that the $C1s$ peak for as-deposited UNCD films is located at 286.8 eV, which is blueshifted in $\Delta V=2.5$ eV with respect to the normal C–C bonds in diamond films (284.3 ± 0.2 eV).[29,30] The blueshift possibly resulted from the electronic traps existing in the UNCD films.[31] In contrast, Fig. 7(b) reveals that the $C1s$ peak for as-deposited MCD films is located at 284.3 eV, which is close to the normal C–C bonds for diamonds, indicating that there exists no surface charge for MCD films. It should be noted that the UNCD films were grown in Ar-plasma, whereas the MCD films were synthesized in H_2-plasma. Therefore, only the dangling bonds in MCD films can be fully compensated so that the surface charges were eliminated. The dangling bonds in UNCD films cannot be efficiently compensated, and large proportion of surface charges were induced, resulting in marked blueshift for $C1s$ peak.

The 100 MeV Ag^{9+}-ion irradiation (5×10^{10} ions/cm^2) will induce some atomic defects, which act as electronic charge traps and result in blueshift for both films.[31] The $C1s$ peak was thus shifted to 287.1 eV for UNCD films and to

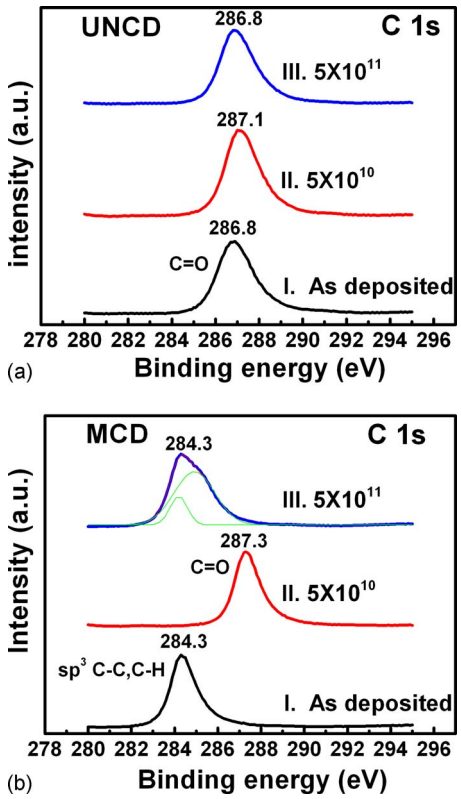

FIG. 7. (Color online) The XPS for as-deposited and 100 MeV Ag^{9+}-ion irradiated (a) UNCD and (b) MCD films.

287.3 eV for MCD films [curve II, Figs. 7(a) and 7(b)]. Increasing the fluence of Ag^{9+}-ion irradiation to 5×10^{11} ions/cm^2 removes some of the electron traps, shifting the *C*1*s* peak toward the normal C–C position. The reduction in electron traps possibly resulted from the healing of atomic defects by the melting and recrystallization effect, which will be discussed shortly. However, such a change in XPS surface characteristics does not correlate very well with the improvement in EFE properties of the films. Detailed microstructure of these films was thus investigated using TEM to understand the genuine factor altering the EFE properties of the films.

Figure 8 shows the typical TEM micrographs of the Ag^{9+}-ion irradiated (5×10^{11} ions/cm^2) UNCD films. The general characteristics of UNCD materials are still preserved, viz., they contain grains with 5–10 nm in size (e.g., region A), whose enlarged micrograph is illustrates as inset of Fig. 8(a). However, aggregation of clusters (~50–100 nm) is induced in some other regions [e.g., region B, Fig. 8(a)]. The enlarged micrograph of region B [Fig. 8(b)] and the associated structural images [insets B_1, B_2, and B_3 in Fig. 8(b)] reveal that the clusters consist of crystalline aggregates with flakelike geometry. The Fourier transformed images in the insets indicate that they are nanosized graphites, implying that phase transformation of the materials has occurred probably via the local melting and recrystallization process.[32] The implication of above-described results is that while low dosage of 100 MeV Ag^{9+}-ion irradiation only induced the formation of atomic defects, high dosage of Ag^{9+}-ion irradiation can induce the melting and recrystallization of the materials

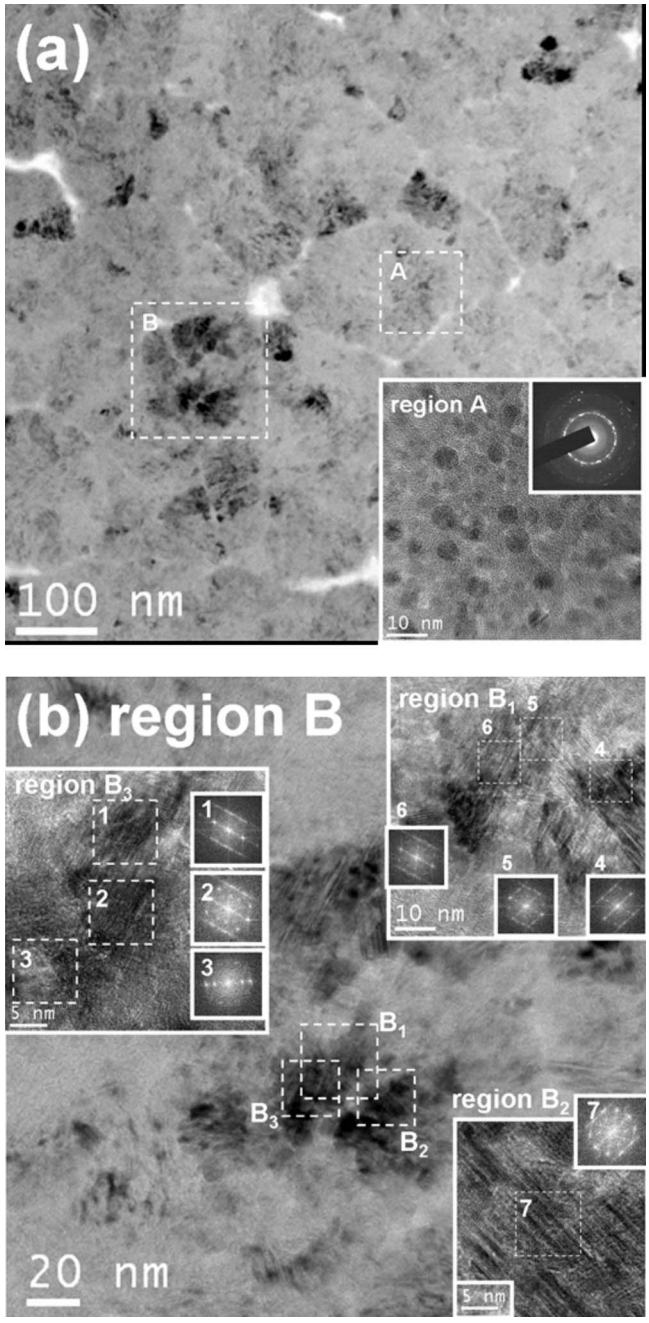

FIG. 8. TEM micrograph for (a) 100 MeV Ag^{9+}-ion irradiated (5×10^{11} ion/cm^2) UNCD films with the inset showing enlarged micrograph of region "A" and (b) the enlarged micrograph of region "B," where the insets B_1, B_2, and B_3 are the structure images with the Fourier transformed images corresponding to designated regions.

along the trajectories of the impinging heavy ions, eliminating the atomic defects. Such a phenomenon is in accord with the previous reports[32] and can account for the blueshift of *C*1*s* peak for low-dose Ag^{9+}-ion irradiated samples and reversed-shift in this peak for high dose Ag^{9+}-irradiated ones.

The effect of 100 MeV Ag^{9+}-ion irradiation on altering the microstructure of the MCD is illustrated in Fig. 9, indicating that most of the grains are of the same microstructure as the pristine MCD films, i.e., they are featureless [Fig. 9(a)]. Occasionally, carbon clusters about 5–10 nm in size were observed preferentially along the grain boundaries, as

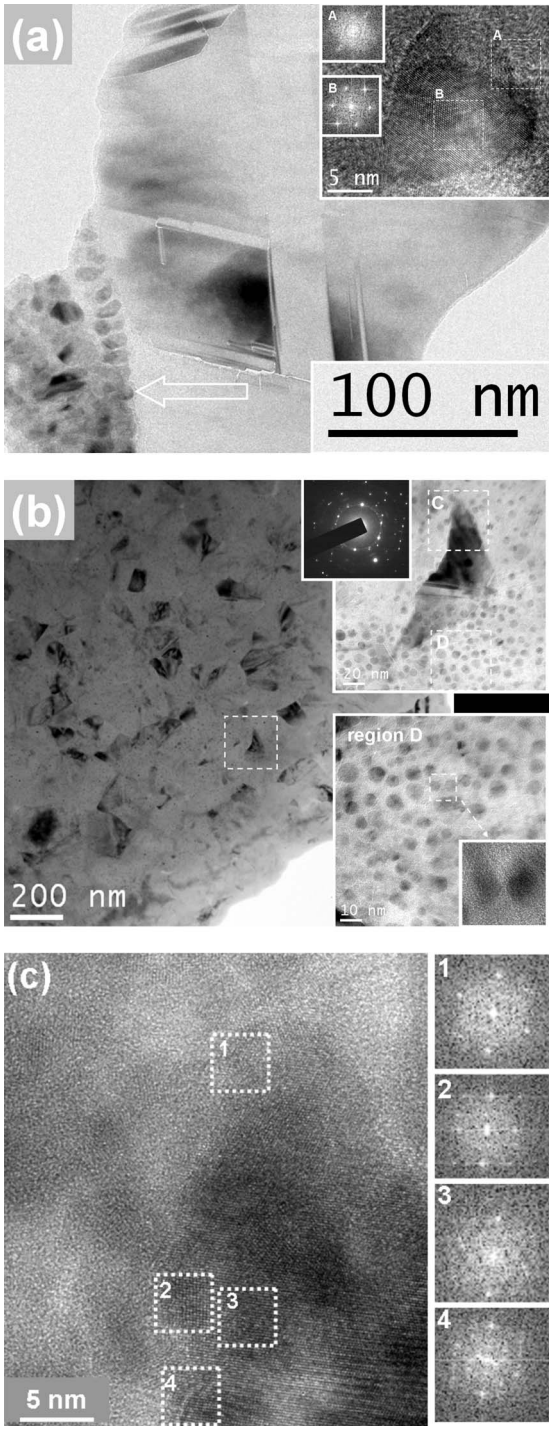

FIG. 9. TEM micrographs for 100 MeV Ag^{9+}-ions irradiation (5×10^{11} ion/cm^2) MCD films: (a) typical granular structure and (b) other regions with inset showing the enlarged micrographs of the designated region. (c) Enlarged micrograph of region C in (b), where the Fourier transformed images 1 and 3 are diamonds and those of 2 and 4 are graphites.

indicated by arrow in Fig. 9(a). Structure image and Fourier transformed micrograph of a typical area in this region [inset, Fig. 9(a)] indicate that the clusters are either nanosized diamonds or nanographites. In a very rare case, a large region of the materials was converted into multiphase mixtures, as shown in Fig. 9(b). The enlarged micrograph shown as inset in this figure reveals that this region contains large crystals (about tens of microns in size) scarcely distributed among the nanosized clusters. The enlarged micrographs for region D [the inset, Fig. 9(b)] and the structure image indicate that the nanosized clusters are diamonds. Figure 9(c) shows structure image of region C, indicating that the clusters are either nanosized diamonds (insets 1 and 3) or nanographites (insets 2 and 4), coexisting with amorphous matrix. Presumably, these nanoclusters are formed by melting and recrystallization of diamond materials in the region where the heavy ions passed through. Restated, the 100 MeV Ag^{9+}-ion irradiation modifies the microstructure of the MCD films in the same manner as that on the UNCD films, viz., the induction of the atomic defects at low dosage and the formation of nanodiamonds (or nanographites) at high dosage via melting and recrystallization process. This observation is in accord with the model proposed by Belykh *et al.*[33]

While the induction of the nanocrystalline clusters is the plausible mechanism improving the EFE properties of the diamond films upon heavy ion irradiation, there still remains one question, that is, why the heavy ion irradiation improved more significantly the EFE properties for the MCD films than that for the UNCD films. Apparently, the probable cause is the different effect on altering the microstructure of the materials induced by the heavy ion irradiation. As mentioned earlier, the grains of MCD films are large (~300–500 nm) and those of UNCD films are extremely small (~5 nm). The trajectories of the energetic heavy ions passing through the large diamond grains of MCD films produced interconnected sp^2-bonded carbon networks and thus led to good electron conducting path through the diamond grains. In contrast, for UNCD films, the melting and recrystallization processes resulted in agglomeration of nanosized grains, which reduced the connectivity of the grain boundaries and decreased the continuity of electron conduction path. Therefore, the improvement in the EFE properties in UNCD films is not as pronounced as that in MCD films.

IV. CONCLUSION

The effect of 100 MeV Ag^{9+}-ions irradiation on MCD and UNCD films have been studied. TEMs revealed that while some regions in the large grains of MCD films were broken up into small clusters, some of the ultrasmall grains of UNCD films were agglomerated. This phenomenon is ascribed to the induction of the melting and recrystallization processes at high fluences. The heavy ion irradiation improved the EFE behavior of the large grain MCD materials more markedly than that on the ultrasmall grain UNCD materials.

ACKNOWLEDGMENTS

The authors would like to thank the National Science Council, Republic of China, for the support of this research through Project No. NSC 96-2112-M032-011-MY3.

[1]F. J. Himpsel, J. A. Knapp, J. A. VanVecten, and D. E. Eastman, Phys. Rev. B **20**, 624 (1979).
[2]W. Zhu, G. P. Kochanski, and S. Jin, Science **282**, 1471 (1998).
[3]B. Dischler, C. Wild, W. Müller-Sebert, and P. Koidl, Physica B **185**, 217 (1993).
[4]P. W. May, M. N. R. Ashfold, and Yu. A. Mankelevich, J. Appl. Phys. **101**,

053115 (2007).
[5]Sh. Michaelson, O. Ternyak, R. Akhvlediani, A. Hoffman, A. Lafosse, R. Azria, O. A. Williams, and D. M. Gruen, J. Appl. Phys. **102**, 113516 (2007).
[6]E. J. Correa, Y. Wu, J. G. Wen, R. Chandrasekharan, and M. A. Shannon, J. Appl. Phys. **102**, 113706 (2007).
[7]C. J. Tang, M. A. Neto, M. J. Soares, A. J. S. Fernandes, A. J. Neves, and J. Grácio, Thin Solid Films **515**, 3539 (2007).
[8]P. W. May, W. J. Ludlow, M. Hannaway, P. J. Heard, J. A. Smith, and K. N. Rosser, Chem. Phys. Lett. **446**, 103 (2007).
[9]S. G. Wang, Q. Zhang, S. F. Yoon, J. Ahn, Q. Wang, Q. Zhou, and D. J. Yang, Phys. Status Solidi A **193**, 546 (2002).
[10]K. H. Wu, E. G. Wang, Z. X. Cao, Z. L. Wang, and X. Jiang, J. Appl. Phys. **88**, 2967 (2000).
[11]S. Prawer and R. Kalish, Phys. Rev. B **51**, 15711 (1995).
[12]J. Krauser, J.-H. Zollondz, A. Weidinger, and C. Trautmann, J. Appl. Phys. **94**, 1959 (2003).
[13]N. Koenigsfeld, H. Hofsass, D. Schwen, A. Weidinger, C. Trautmann, and R. Kalish, Diamond Relat. Mater. **12**, 469 (2003).
[14]S. Prawer, A. Hoffman, and R. Kalish, Appl. Phys. Lett. **57**, 2187 (1990).
[15]W. Zhu, G. P. Kochanski, S. Jin, L. Seibles, D. C. Jacobson, M. McCormac, and A. E. White, Appl. Phys. Lett. **67**, 1157 (1995).
[16]N. Dilawar, R. Kapil, V. D. Vankar, D. K. Avasthi, D. Kabiraj, and G. K. Mehta, Thin Solid Films **305**, 88 (1997).
[17]A. Dunlop, G. Jaskierowicz, P. M. Ossi, and S. Della-Negra, Phys. Rev. B **76**, 155403 (2007).
[18]P. T. Pandey, G. L. Sharma, D. K. Awasthi, and V. D. Vankar, Vacuum **72**, 297 (2004).
[19]P. M. Koinkar, R. S. Khairnar, S. A. Khan, R. P. Gupta, D. K. Avasthi, and M. A. More, Nucl. Instrum. Methods Phys. Res. B **244**, 217 (2006).
[20]Y. C. Lee, S. J. Lin, I. N. Lin, and H. F. Cheng, J. Appl. Phys. **97**, 054310 (2005).
[21]Y. H. Chen, C. T. Hu, and I. N. Lin, J. Appl. Phys. **84**, 3890 (1998).
[22]J. F. Ziegler, J. P. Biersack, and U. Littmark, *The Stopping and Ranges of Ions in Solids* (Pergamon, New York, 1985).
[23]R. H. Fowler and L. Nordheim, Proc. R. Soc. London, Ser. A **119**, 173 (1928).
[24]A. C. Ferrari and J. Robertson, Phys. Rev. B **63**, 121405 (2001).
[25]R. G. Buckley, T. D. Moustakas, L. Ye, and J. Varon, J. Appl. Phys. **66**, 3595 (1989).
[26]X. Xiao, J. Birrel, J. E. Gerbi, O. Auciello, and J. A. Carlisle, J. Appl. Phys. **96**, 2232 (2004).
[27]S. Bhattacharyya, O. Auciello, J. Birrell, J. A. Carlisle, L. A. Curtiss, A. N. Goyette, D. M. Gruen, A. R. Krauss, J. Schlueter, A. Sumant, and P. Zapol, Appl. Phys. Lett. **79**, 1441 (2001).
[28]A. Laikhtman, I. Gouzman, A. Hoffman, G. Comtet, L. Hellner, and G. Dujardin, J. Appl. Phys. **86**, 4192 (1999).
[29]J. T. Titantah and D. Lamoen, Carbon **43**, 1311 (2005).
[30]C. Popov, W. Kulisch, S. Boycheva, K. Yamamoto, G. Ceccone, and Y. Koga, Diamond Relat. Mater. **13**, 2071 (2004).
[31]P. T. Joseph, N. H. Tai, C. Y. Lee, H. Niu, W. F. Pong, and I. N. Lin, J. Appl. Phys. **103**, 043720 (2008).
[32]F. F. Komarov, Phys. Usp. **46**, 1253 (2003).
[33]T. A. Belykh, A. L. Gorodishchensky, L. A. Kazak, V. E. Semyannikov, and A. R. Urmanov, Nucl. Instrum. Methods Phys. Res. B **51**, 242 (1990).